Pis'ma v ZhETF, vol. 93, iss. 2, pp. 95 – 100 © 2011 January 25

Observation of Multi-Gap Superconductivity in GdO(F)FeAs by Andreev Spectroscopy

T. E. Shanygina[▽*1)], Ya. G. Ponomarev[*], S. A. Kuzmichev[*], M. G. Mikheev[*], S. N. Tchesnokov[*], O. E. Omel'yanovskii[▽+], A. V. Sadakov[▽+], Yu. F. Eltsev[▽], A. S. Dormidontov[▽], V. M. Pudalov[▽△], A. S. Usol'tsev[▽△], E. P. Khlybov[□+]

[▽] P.N. Lebedev Physical Institute RAS, 119991 Moscow, Russia

[*] Department of Low Temperature Physics and Superconductivity, Moscow State University, 119991 Moscow, Russia

[+] International Laboratory of High Magnetic Fields and Low Temperatures, 53-421 Wroclaw, Poland

[△] Moscow Institute of Physics and Technology, 141700 Moscow, Russia

[□] Institute for High Pressure Physics RAS, 142190 Troitsk, Moscow district, Russia

Submitted 9 December 2010

We have studied current-voltage characteristics of Andreev contacts in polycrystalline $GdO_{0.88}F_{0.12}FeAs$ samples with bulk critical temperature $T_c = (52.5 \pm 1)$ K using break-junction technique. The data obtained cannot be described within the single-gap approach and suggests the existence of a multi-gap superconductivity in this compound. The large and small superconducting gap values estimated at $T = 4.2$ K are $\Delta_L = 10.5 \pm 2$ meV and $\Delta_S = 2.3 \pm 0.4$ meV, respectively.

Novel superconducting compounds of 1111 family based on rare-earth oxypnictides REOFeAs (RE = La, Sm, Gd etc.) [1, 2] are currently in the focus of research interest. Some of their features such as layered structure and spatial separation of the carrier reservoir layers and the superconducting pairing layers are similar to those of cuprates. However, many other properties differ substantially and promise new interesting physics [3]. At present, the key issues under investigations are the effect of various types of doping, pairing mechanism, symmetry of the order parameter, quasiparticle energy spectrum, and the superconducting energy gap(s).

The stoichiometric compounds of the 1111-family are antiferromagnetic metals with spin density wave ground state [4]. Partial deficiency of oxygen or fluorine substitution for oxygen induces superconductivity in the FeAs-layers. Replacement of rare-earth elements also affects the superconducting critical temperature, T_c. In particular, T_c of Gd-based oxypnictide may be lowered by partial replacement of Y for Gd [5] or gained up by introducing Th instead of Gd [6]. T_c=56 K found in $Gd_{0.8}Th_{0.2}OFeAs$ compound is today the highest one for iron-based superconductors.

According to band structure calculations, the total density of states at the Fermi level $N(0)$ is formed mainly by Fe 3d-states [7 – 9]. As shown in Ref. [10], the T_c values for different iron-based superconductors correlate with $N(0)$, thus giving support to the BCS-like coupling in these compounds.

The theoretically calculated Fermi surface for 1111-system [11 – 13] consists of quasi-two-dimensional (2D) hole sheets centered at the Γ point and two electron sheets at the M points of the first Brillouin zone. Within the so called minimal two-band model, these four bands may be considered as two effective 2D bands [14, 15]. Correspondingly, many of the available theoretical and experimental data indicate that iron-based layered materials are multiband superconductors with s-type symmetry of the order parameter [3]. Knight shift measurements in 1111-class compounds [16] have proven unambiguously the spin-singlet type pairing in these materials. Several data were reported in favor of $s^{\pm}$ [17, 18] or s^{++} order parameter symmetry [19], making the experimental situation regarding 1111-compounds uncertain.

The magnitude and structure of the superconducting gap Δ is intimately related to the pairing mechanism. ARPES measurements are not sensitive enough to resolve unambiguously such fine details as Δ, on the scale of a few meV, that makes this parameter accessible nearly exclusively from point contact spectroscopy, such as scanning tunneling spectroscopy (STS), tunneling- and point-contact Andreev reflection (PCAR) spectroscopy (the latter in the regime of SN-, or symmetrical SNS-junctions). The available experimental reports are however rather inconsistent for 1111 class compounds [20 – 23], even for the most intensively stud-

[1)] e-mail: tatiana.shanygina@gmail.com

ied SmO(F)FeAs. Various types of conclusions have been reported including d-wave like, single gap-like, and multi-gap behavior.

The ambiguity of the experimental information is partly due to an inevitable inhomogeneity of the 1111-type polycrystalline samples and lack of large size 1111-type single-crystals suitable for these measurements. Another cause for the divergency of the point contact spectroscopy data is inherent in those experimental techniques, where the sample surface is not cleaved in high vacuum or cryogenic environment. In order to resolve the experimental ambiguity, evidently, novel sets of comprehensive experimental data are needed, which would comprise self-consistency check, substantial statistics and provide local probing at various points of the in-situ cleaved surfaces.

Here we report the superconducting gap measurements in nearly optimally doped $GdO_{0.88}F_{0.12}FeAs$ samples by SNS Andreev spectroscopy using the break-junction technique [24]. Until now these measurements have not been done for Gd-1111, an analogue to Sm-1111 with approximately the same $T_c \sim 53\,\mathrm{K}$. The break junction technique opens a nice opportunity to prepare in helium atmosphere, at liquid ^{4}He temperatures, clean surfaces forming Andreev contact. Another advantage is a possibility of fine mechanical readjusting the contact during experiment and, thus, to collect multiple data from different local areas of the same sample. Using this method we have unambiguously detected the presence of two superconducting gaps, whose best fit values averaged over about 30 spectra are $\Delta_L = 10.5 \pm 2\,\mathrm{meV}$ and $\Delta_S = 2.3 \pm 0.4\,\mathrm{meV}$ at $T = 4.2\,\mathrm{K}$.

Polycrystalline samples GdO(F)FeAs were prepared by high pressure synthesis [25]. The chips of high purity Fe, and powders of single-phase FeF_3, Fe_2O_3, and GdAs were mixed together in the nominal ratio and pressed into pellets of 3 mm diameter and 3 mm height. The pellets were placed in boron nitride crucible and synthesized at pressure of 50 kb and temperature 1350 °C during 60 min. The X-ray diffraction pattern averaged over the sample area showed a polycrystalline compound with a dominating desired 1111-phase (with lattice parameters $a = 3.902(2)$ Å, $c = 8.414(5)$ Å) and an admixture of incidental FeAs and Gd_2O_3 phases. The subsequent local EDS analysis (JSM-7001FA) has revealed that the incidental phases are concentrated in grains of about 1 mkm size which are scattered in the bulk majority phase. This fact opens a possibility to probe properties of the true majority phase using local techniques, such as PCAR. Superconducting properties of the samples were tested by measurements of temperature dependence of ac-magnetic susceptibility and resistivity $R(T)$. Both showed a sharp superconducting transition in our polycrystalline samples with $T_c \approx 52.5\,\mathrm{K}$ (the latter value was defined at a maximum of $dR(T)/dT$-curve). Figure 1 shows typical temperature dependence of resistance and its derivative.

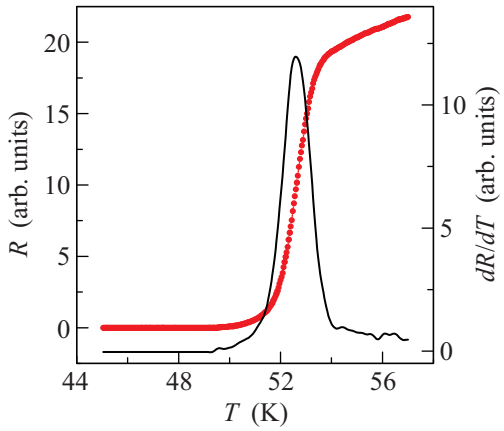

Fig.1. Superconducting transition for polycrystalline $GdO_{0.88}F_{0.12}FeAs$ sample measured prior a microcrack formation (dots). The bulk $T_c = (52.5 \pm 1)\,\mathrm{K}$ was determined at a maximum in $dR(T)/dT$-curve (solid line)

For point-contact spectroscopy we used two methods: (i) multiple Andreev reflections spectroscopy of individual superconductor-constriction-superconductor Sharvin-type contacts [26–28] and (ii) intrinsic Andreev specrtoscopy of stack contacts that usually exist due to the presence of steps and terraces on clean cryogenic cleaves in layered crystals.

Thin plates of about $2 \times 1 \times 0.12\,\mathrm{mm}$ in size were cut from the synthesized pellets. At room temperature, the plate-like sample was mounted onto an elastic bronze holder and the two current and two potential leads were attached to the sample by liquid In-Ga alloy. The holder with the sample was placed in the measuring cell and cooled down to 4.2 K. A microcrack in the sample was generated by precise bending the sample holder at $T = 4.2\,\mathrm{K}$ using a micrometric screw.

Current-voltage dependence, $I(V)$, and its derivative, $dI(V)/dV$, were measured automatically using the 16-bit digital board. The amplitude of a low-level 820 Hz modulation voltage at potential leads of a sample was maintained stable using a lock-in nanovoltmeter (operated as null- detector) and a computer controlled digital bridge with a proportional-integral-derivative feedback signal. As a result, the differential conductance of a contact was proportional to the amplitude of the ac feedback current through the contact.

Figure 2 represents $I(V)$, $dI(V)/dV$ and $d^2I(V)/dV^2$ characteristics for individual An-

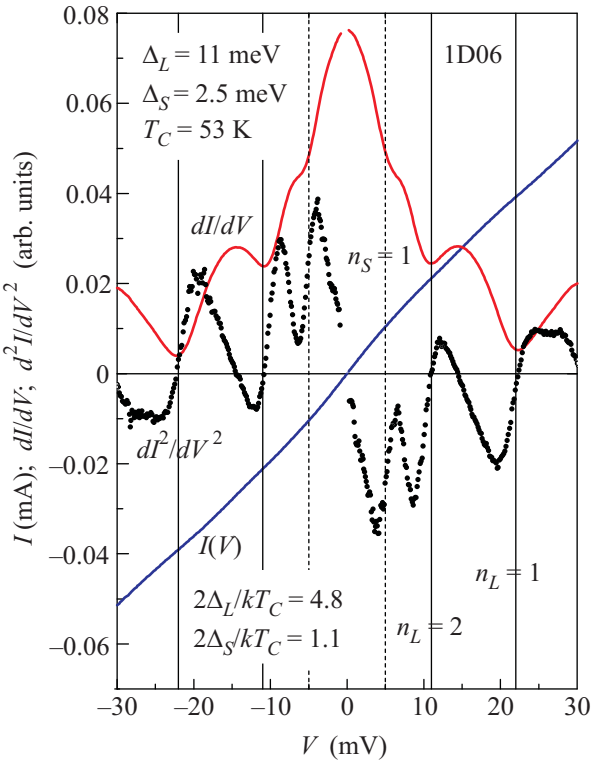

Fig.2. $I(V)$, $dI(V)/dV$ and $d^2I(V)/dV^2$-curves for a single SNS-contact 1D06 at $T = 4.2$K. Background (a polynomial function) is subtracted. The set of dips in the differential conductance at bias voltages $V_{nL} = 2\Delta_L/en$ (vertical solid lines) determines the energy of the large superconducting gap, $\Delta_L \approx 11$ meV. Peculiarities on the $dI(V)/dV$ and $d^2I(V)/dV^2$-curves, marked by dashed lines, indicate the presence of small superconducting gap, $\Delta_S \approx 2.5$ meV

dreev (SNS) break-junction in polycrystalline $GdO_{0.88}F_{0.12}FeAs$ sample measured at $T = 4.2$ K. The observed experimental IV-curves are typical for the clean classical SNS-contacts with excess-current characteristics [27, 29], therefore, the theoretical model of Kümmel et al. [27] is supposed to be applicable to our break-junctions. According to the Kümmel model, the IV-characteristics at low bias voltages should show a subharmonic gap structure (SGS) with a series of dips in the dynamic conductance $dI(V)/dV$ at bias voltages

$$V_n = 2\Delta/en, \qquad (1)$$

with an integer $n = 1, 2...$, due to multiple AR effect. For a two-gap superconductor, two independent SGSs corresponding to the large Δ_L and small Δ_S gaps are anticipated.

The dips labeled on Figure 2 as $n_L = 1$ and 2 on SGS reflect the large gap; they are marked with vertical solid lines. The singularities shown by vertical dashed lines cannot be attributed to the large gap and, therefore, may reflect the existence of a small gap $\Delta_S \approx 2.5$ meV. Comparing the result for the large gap (Fig.2) with Eq. (1) one can easily obtain $\Delta_L \approx 11$ meV.

By readjusting the contact, we could observe clear sets of dips on $dI(V)/dV$ curve due to either large- or small-gaps, or even to both (as shown in Fig.2). Figure 3 expands the small bias range, where the subharmonics of

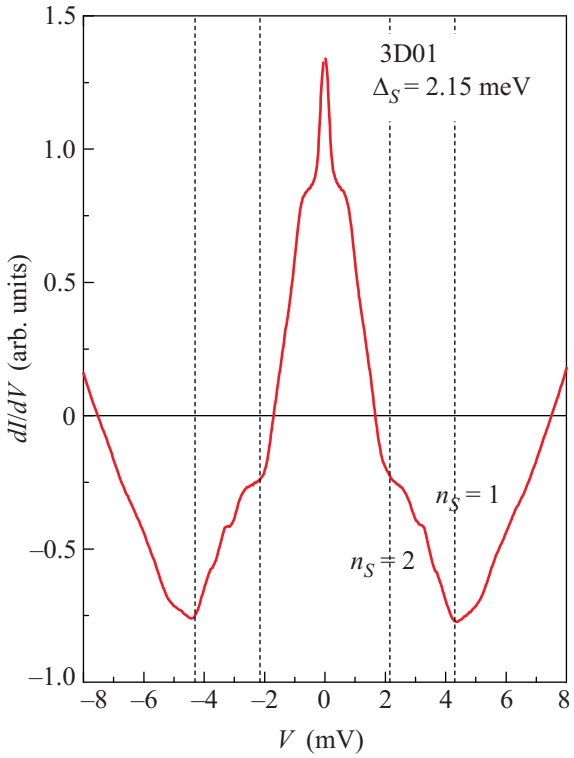

Fig.3. Differential conductance of the SNS contact 3D01 in $GdO_{0.88}F_{0.12}FeAs$ sample at $T = 4.2$K. Background is subtracted. Two differential conductance dips define the energy of the small superconducting gap $\Delta_S \approx 2.15$ meV. The anticipated bias voltages $V_{nS} = 2\Delta_S/en$ are depicted by vertical dashed lines

the small gap are clearly seen in dI/dV curves for a single SNS-contact 3D01. For clarity, the smoothly varying background is subtracted. Using expression (1), from the set of differential conductance dips on the $dI(V)/dV$ curve we determined the energy of the small superconducting gap $\Delta_S = 2.15$ meV. In Fig.3, one can also see two extra features at ≈ 3 mV and 3.7 mV, which can not be attributed to either large or small gap subharmonics. They may be caused by excitation of collective modes and require additional studies.

The peculiarities in the $dI(V)/dV$ and $d^2I(V)/dV^2$-characteristics shown in Figs. 2 and 3 clearly manifest the existence of two gaps in our GdO(F)FeAs samples. This behavior is similar to that observed ear-

lier in the multi-band superconductor $Mg_{1-x}Al_xB_2$ [30] and in $LaO_{0.9}F_{0.1}FeAs$ [31] (an analog to our Gd-1111 sample with somewhat lower $T_c \approx 28$ K). The sharpest SGS (like those in Fig.3) may be usually observed only on $dI(V)/dV$-characteristics of Andreev contacts of the high quality and of small size, comparable to the quasiparticles mean free path (ballistic limit) [28]. For such a case, a number of the observable gap peculiarities (up to 4 in some samples) facilitates interpretation of the multigap subharmonic structure.

Our experimental data are summarized in Figure 4 where the normalized to a single junction bias voltages

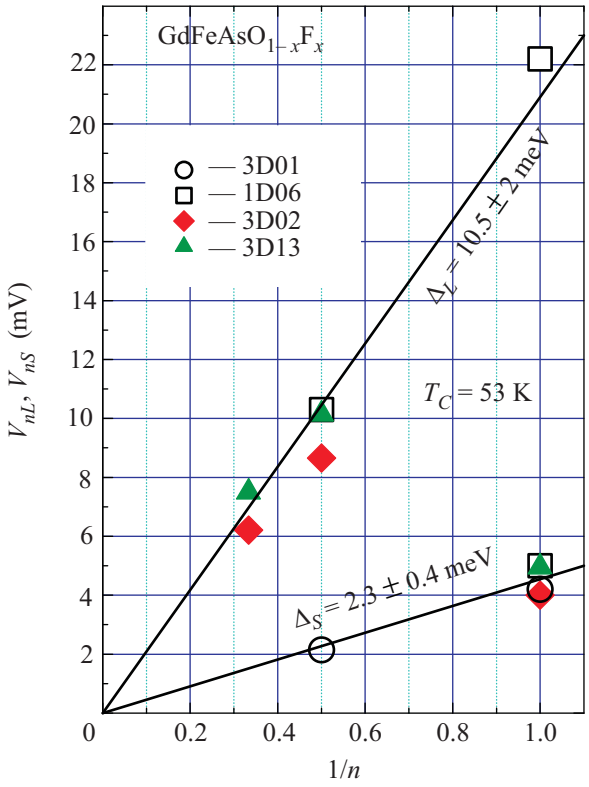

Fig.4. Normalized bias voltages $V_n = 2\Delta_{L,S}/en$ versus $1/n_{L,S}$ for the studied SNS-arrays. The averaged values of the superconducting gaps are $\Delta_L = (10.5 \pm 2)$meV and $\Delta_S = (2.3 \pm 0.4)$meV. Solid lines are guides to the eye

$V_{nL,S}$ for five microcontacts are plotted versus $1/n_{L,S}$. According to expression (1), such dependences have to fall onto straight lines passing through zero. This is indeed fulfilled for Δ_L in all samples; for Δ_S, this however, could be verified only in sample 3D01, because a rich picture of reproducible features detected at low bias voltages impeded the analysis for other samples.

Based on the data obtained we conclude on the existence of two distinct superconducting gaps with energies $\Delta_L = (10.5 \pm 2)$ meV and $\Delta_S = (2.3 \pm 0.4)$meV at $T = 4.2$K in $GdO_{1-x}F_xFeAs$ sample. The reproducibility of two SGSs detected at $dI(V)/dV$-characteristics of various Andreev arrays, formed by the break- junction technique, support this conclusion. In some cases we observed extra features in dI/dV-curves signalling the existence of the 3rd, smaller gap, $\Delta_{SS} \sim 1$ meV.

Using the determined gap energies and bulk $T_c = (52.5 \pm 1)$K, one can estimate $2\Delta/k_BT_c$ ratio. For the large gap, our experimental data lead to $2\Delta_L/k_BT_c = (4.8 \pm 1.0)$ that exceeds the standard BCS value, 3.52, for single-gap superconductors in the weak coupling limit. This fact together with rather conventional exponent value for Fe isotope effect [32] resembles the BCS – model behavior with strong electron-phonon coupling. At the same time, the $2\Delta/k_BT_c$ ratio for the small gap $2\Delta_S/k_BT_c \approx 1.1 < 3.52$ suggests that the "weak" superconductivity may be induced by interband coupling, due to k-space internal proximity effect between two condensates, where the large gap condensate plays the "driving" role. In particular, similar situation is believed to be realized in MgB_2 [30] and $LaO_{0.9}F_{0.1}FeAs$ [31].

Summary of the Δ values (in meV) measured for 1111-family REO(F)FeAs compounds by point contact Andreev reflection (PCAR), break-junction Andreev reflection (BJ), scanning tunneling spectroscopy technique (STS), and ARPES

RE	T_c(K)	method	Δ_L	Δ_S	ref.
Gd	53	BJ	10.5±2	2.3±0.4	this work
Sm	53	ARPES	15±1.5	no	[34]
Sm	52	PCAR	18±3	6.15±0.45	[35]
Sm	52	PCAR	19	5.7	[36]
Sm	52	STS	8–8.5	no	[21]
Sm	51.5	PCAR	20	6.6	[36]
Sm	51	PCAR	10	4	[22]
Nd	51	PCAR	14±1	6±1	[37]
Nd	51	PCAR	12.5±0.5	6.3±0.3	[38]
Nd	48	BJ,STS	7–10	no	[33]
Tb	45	PCAR	8.8	5	[39]
Nd	45	PCAR	11±2	5±1	[40]
Sm	42	PCAR	15±1	4.9±0.5	[35]
Sm	42	PCAR	6.7±0.1	no	[18]

The presence of the large superconducting gap characterized by $2\Delta_L/k_BT_c > 3.52$ in the 1111-family compounds REOFeAs (RE = La, Sm, Nd) was confirmed by tunneling spectroscopy using break-junction technique [33], point-contact Andreev reflection spectroscopy [20, 22, 33 – 40] scanning tunneling spectroscopy [21, 33], and angle-resolved photoemission spectroscopy (ARPES) [34] (see Table). To the best of our knowledge, there is no other available data for

Gd-1111. Therefore, we compare in Table 1 our data for Gd-1111 with other data available for Sm-, Nd- and Tb-1111 superconductors with similar T_c. We emphasize rather good agreement between $2\Delta_L/k_BT_c$ values determined from our study and those from STS [21], break-junction measurements [33], and some PCAR-measurements [22, 38 – 49].

As to the small gap, there is evidently a sizeable spread in its value $(2-5)$ meV observed in different experiments. We can not also exclude that the spread may be caused by the existence of three-gap superconductivity in 1111-system with multiple-sheet Fermi surface [13, 41]; for the smallest gap, we estimate $2\Delta_S/k_BT_c \approx \approx 0.5$.

In conclusion, we have studied the $I(V)$- and $dI(V)/dV$-characteristics at $T = 4.2$ K for various SNS Andreev break-junctions in polycrystalline $GdO_{0.88}F_{0.12}FeAs$ samples with bulk critical temperatures $T_c \approx 52.5$ K. The obtained characteristics do not follow the standard single-gap model behavior. Two clearly observed independent subharmonic gap structures point at the existence of two distinct superconducting gaps, $\Delta_L = (10.5 \pm 2)$ meV and $\Delta_S = (2.3 \pm 0.4)$ meV determined at $T = 4.2$K. The estimated $2\Delta_L/k_BT_c$ ratio exceeds the standard BCS value, 3.52, for single-gap superconductors and weak-coupling limit while for the small gap the $2\Delta/T_c$-ratio $2\Delta_S/k_BT_c < 3.52$.

The authors are grateful to E.G. Maksimov, E.V. Antipov, and S.M. Kazakov for valuable discussions and S.M. Kazakov for help in X-ray diffraction characterization of the samples. The work was partially supported by the Russian Foundation for Basic Research and by the Russian Ministry for Education and Science.

1. Y. Kamihara, H. Hiramatsu, M. Hirano et al., J. Am. Chem. Soc. **128**, 10012 (2006).
2. Y. Kamihara, T. Watanabe, M. Hirano, and H. Hosono, J. Am. Chem. Soc. **130**, 3296 (2008).
3. For a review, see: D.C. Johnston, Adv. Phys. **59**, 803 (2010); M.V. Sadovskii, Physics-Uspekhi **51**, 1201 (2008).
4. H.H. Klauss, H. Luetkens, R. Klingeler et al., Phys. Rev. Lett. **101**, 077005 (2008); H. Luetkens, H. H. Klauss, R. Khasanov et al., Phys. Rev. Lett. **101**, 097009 (2008).
5. K. Kadowaki, A. Goya, T. Mochiji, and S. V. Chong, J. Phys.: Conf. Ser. **150**, 052088 (2009).
6. C. Wang, L. Li, S. Chi et al., Europhys. Lett. **83**, 67006 (2008).
7. I.A. Nekrasov, Z.V. Pchelkina, and M.V. Sadovskii, Pis'ma v ZhETF, **87**, 647 (2008).
8. H. Eschrig and K. Koepernik, arXiv:0905.4844v1.
9. T. Miyake, K. Nakamura, R. Arita, and M. Imada, J. Phys. Soc. Jpn. **79**, 044705 (2010).
10. M.V. Sadovskii, E.Z. Kuchinskii, and I.A. Nekrasov, Pis'ma v ZhETF **91**, 567 (2010) [JETP Lett. **91**, 518 (2010)].
11. D.J. Singh and M.H. Du, Phys. Rev. Lett. **100**, 237003 (2008); D.J. Singh, Physica C **469**, 418 (2009).
12. I.A. Nekrasov, Z.V. Pchelkina, and M. V. Sadovskii, Pis'ma v ZhETF **88**, 155 (2008) [JETP Lett. **88**, 144 (2008)].
13. A.I. Coldea, J.D. Fletcher, A. Carrington et al., Phys. Rev. Lett. **101**, 216402 (2008).
14. S. Raghu, X.-L. Qi, C.-X. Liu et al., Phys. Rev. B **77**, 220503(R) (2008).
15. J. Li and Y. P. Wang, Chin. Phys. Lett. **25**, 2232 (2008).
16. H. Mukuda, N. Terasaki, M. Yashimaa et al., Physica C **469**, 559 (2009).
17. Yu-R. Zhou, Y.-R. Li, J.-W. Zuo et al., arXiv:0812.3295.
18. C.-T. Chen, C.C. Tsuei, M.B. Ketchen et al., Nature Physics **6**, 260 (2010).
19. I.I. Mazin and J. Schmalian, arXiv: 0901.4790.
20. T.Y. Chen, Z. Tesanovic, R.H. Liu et al., Nature **453**, 1224 (2008).
21. O. Millo, I. Asulin, O. Yuli et al., Phys. Rev. B **78**, 092505 (2008).
22. Y.-L. Wang, L. Shan, L. Fang et al., Supercond. Sci. Technol. **22**, 015018 (2009).
23. M.H. Pan, X.B. He, G.R. Li et al., arXiv: 0808.0895.
24. J. Müller, J.M. van Ruitenbeek, and L.J. de Jongh, Physica C **191**, 485 (1992).
25. E.P. Khlybov, O.E. Omelyanovsky, A. Zaleski et al., Pis'ma v ZhETF **90**(5), 429 (2009) [JETPL **90**, 387 (2009)].
26. A.F. Andreev, Zh. Eksp. Teor. Fiz. **46**, 1823 (1964). [Soviet Phys. JETP **19**, 1228 (1964)].
27. R. Kümmel, U. Gunsenheimer, and R. Nicolsky, Phys. Rev. B **42**, 3992 (1990).
28. Yu. V. Sharvin, Zh. Eksp. Teor. Fiz. **48**, 984 (1965).
29. B.A. Aminov, A.A. Golubov, and M.Yu. Kupriyanov, Phys. Rev. B **53**, 365 (1996).
30. Ya.G. Ponomarev, S.A. Kuzmichev, M.G. Mikheev et al., Sol. State Comm. **129**, 85 (2004); Ya.G. Ponomarev, S.A. Kuzmichev, N.M. Kadomtseva et al., Pis'ma v ZhETF, **79**, 597 (2004) [JETP Lett. **79**, 484 (2004)]; Ya.G. Ponomarev, S.A. Kuzmichev, M.G. Mikheev et al., Pis'ma v ZhETF, **85**, 52 (2007) [JETP Lett. **85**, 46 (2007)].
31. Ya.G. Ponomarev, S.A. Kuzmichev, M.G. Mikheev, Phys. Rev. B **79**, 224517 (2009).
32. R.H. Liu, T. Wu, G. Wu et al., Nature **459**, 64 (2009).
33. T. Ekino, A. Sugimoto, H. Okabe et al., Physica C (2009, in press), doi:10.1016/j.physc.2009.10.079; A. Sugimoto, T. Ekino, R. Ukita et al., Physica C **470**, 1070 (2010).

34. T. Kondo, A. F. Santander-Syro, O. Copie et al., Phys. Rev. Lett. **101**, 147003 (2008).
35. D. Daghero, M. Tortello, R. S. Gonnelli et al., Phys. Rev. B **80**, 060502(R) (2009).
36. R. S. Gonnelli, D. Daghero, M. Tortello et al., Physica C 469, **512** (2009).
37. N. Miyakawa, M. Minematsu, S. Kawashima et al., J. Supercond. Novel Magn. **23**, 575 (2010).
38. M. Tanaka and D. Shimada, J. Supercond. Novel Magn. (2010, original paper), doi:10.1007/s10948-010-0869-7.
39. K. A. Yates, L. F. Cohen, Zhi-An Ren et al., New J. Phys. **11**, 025015 (2009).
40. P. Samuely, P. Szabo, Z. Pribulova et al., Supercond. Sci. Technol. **22**, 014003 (2009).
41. S. Lebegue, Z. P. Yin, and W. E. Pickett, New J. of Phys. **11**, 025004 (2009).